A discrete-time scheduling model for continuous power-intensive process networks with various power contracts

Qi Zhang[a], Arul Sundaramoorthy[b], Ignacio E. Grossmann[a,*], Jose M. Pinto[c]

[a] *Center for Advanced Process Decision-making, Department of Chemical Engineering, Carnegie Mellon University, Pittsburgh, PA 15213, USA*
[b] *Praxair, Inc., Business and Supply Chain Optimization R&D, Tonawanda, NY 14150, USA*
[c] *Praxair, Inc., Business and Supply Chain Optimization R&D, Danbury, CT 06810, USA*

Abstract

Increased volatility in electricity prices and new emerging demand side management opportunities call for efficient tools for the optimal operation of power-intensive processes. In this work, a general discrete-time model is proposed for the scheduling of power-intensive process networks with various power contracts. The proposed model consists of a network of processes represented by Convex Region Surrogate models that are incorporated in a mode-based scheduling formulation, for which a block contract model is considered that allows the modeling of a large variety of commonly used power contracts. The resulting mixed-integer linear programming model is applied to an illustrative example as well as to a real-world industrial test case. The results demonstrate the model's capability in representing the operational flexibility in a process network and different electricity pricing structures. Moreover, because of its computational efficiency, the model holds much promise for its use in a real industrial setting.

Keywords: Production scheduling, demand side management, process networks, power contracts, mixed-integer linear programming

1. Introduction

With deregulated electricity markets and increasing penetration of intermittent renewable energy into the electricity supply mix, the level of uncertainty in the power grid has increased tremendously. This has led to highly volatile electricity prices, which pose immense challenges to the power-intensive industries, such as air separation, aluminum, and chlor-alkali manufacturing. Demand Side Management (DSM), which refers to electric energy management on the consumers' side, has the potential of both significantly reducing the electricity cost

*Corresponding author
Email address: grossmann@cmu.edu (Ignacio E. Grossmann)

for the consumer as well as improving the efficiency and reliability of the power grid.

Only in recent years, the high potential benefits of DSM for the chemical processing industry have been acknowledged by researchers and practitioners (Paulus and Borggrefe, 2011; Samad and Kiliccote, 2012; Merkert et al., 2014). One main concept of industrial DSM is to use the operational flexibility of the plant, which consumes a large amount of power, to take advantage of time-sensitive electricity prices (Charles River Assosicates, 2005; Albadi and El-Saadany, 2008). This can be achieved, for example, by shifting the production to low-price hours; however, load shifting has to be well-considered since one still has to satisfy process constraints and meet product demand. The strong time component in DSM calls for effective scheduling tools that consider the constraints on the production process as well as the price structures and purchasing limitations for different power sources.

Production scheduling has been an active area of research in process systems engineering (PSE) since the late 1970s. Since then, much progress has been made in the modeling of both batch and continuous scheduling problems as well as in the development of efficient methods for solving these models. Numerous general scheduling models have been proposed, many of which are based on the concepts of state-task network (STN) (Kondili et al., 1993; Shah et al., 1993) or resource-task network (RTN) (Pantelides, 1994). For recent reviews of works on production scheduling in PSE, we refer to Méndez et al. (2006), Maravelias (2012), and Harjunkoski et al. (2014).

In recent years, scheduling frameworks for DSM have been proposed for various industrial power-intensive processes such as steelmaking (Ashok, 2006; Castro et al., 2013), electrolysis (Babu and Ashok, 2008), cement production (Vujanic et al., 2012), and air separation (Ierapetritou et al., 2002; Karwan and Keblis, 2007; Zhang et al., 2014b). Castro et al. (2009, 2011) present RTN-based discrete-time and continuous-time models for the scheduling of continuous plants under variable electricity cost. For the same purpose, Mitra et al. (2012) have developed a scheduling model based on the concept of operating modes, which eases the systematic modeling of operational transitions. The resulting mixed-integer linear programming (MILP) model is computationally very efficient, and therefore allows the solution of large-scale industrial problems. However, in the proposed approach, a surrogate model is created for the plant as a whole, which does not explicitly consider interactions between different processes in the plant. Also, the model only considers day-ahead electricity prices and does not take purchasing electricity from pre-agreed power contracts into account.

In this work, we extend the model proposed by Mitra et al. (2012) and further generalize it such that it can be applied to continuous process networks subject to various power contracts. In order to achieve this goal, we explicitly model the process network, in which processes are connected by material flows, and each process is represented by a so-called Convex Region Surrogate (CRS) model. To this process network, the mode-based scheduling formulation is applied as well as a block contract formulation to incorporate different types of power contracts.

The remainder of this paper is organized as follows. In Section 2, the prob-

lem statement is presented before the MILP model is developed in Section 3. The proposed model is applied to an illustrative example and an industrial air separation case study as shown in Sections 4 and 5, respectively. Finally, in Section 6, we close with a summary of the results and some concluding remarks.

2. Problem statement

We consider process networks involving continuous processes which consume significant amount of electric power during operation. Here, a process can refer to a piece of equipment, a set of multiple interconnected pieces of equipment, or an entire plant. The processes in such a process network differ in their feeds and products, the restrictions on the production rates, and the power consumption characteristics. Inventory capacities are given for storable intermediate and final products. Also, for all final products, the demand is given.

Electricity can be purchased from various power contracts which may differ in price, availability, and penalty for under- or overconsumption. We assume that the prices and other conditions for negotiated contracts are known in advance, and that accurate forecasts for the day-ahead or real-time electricity prices are available.

The goal is to find a production schedule over a given scheduling horizon that minimizes the total electricity cost while satisfying all product demand. For every time period of the scheduling horizon, we determine

- the mode of operation for each process,
- the processing rate in each process,
- the material flows in the process network,
- the amount of intermediate and final products stored,
- the amount of power purchased from each power contract.

3. Model formulation

We propose an MILP scheduling model, for which the mathematical formulation is presented below. Note that all continuous variables in this model are constrained to be nonnegative. A list of indices, sets, parameters, and variables is given in the Nomenclature section.

3.1. Time representation

A discrete-time framework is applied in which the time horizon is divided into time periods of equal length, Δt. The notation for the time discretization is such that time period t starts at time point $t-1$ and ends at time point t. The scheduling horizon is defined by the set of time periods $\overline{T} = \{1, 2, \ldots, t^f\}$. $\overline{T}$ is a subset of $T = \{-\theta^u + 1, -\theta^u + 2, \ldots, 0, 1, \ldots, t^f\}$, which also includes time periods in the past that are used in some constraints involving multiple time periods. The common-grid representation is illustrated in Figure 1.

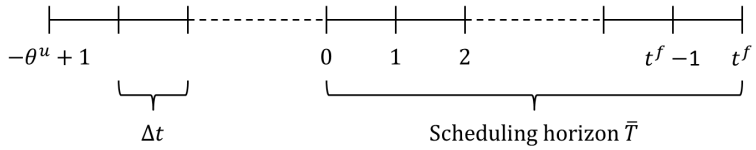

Figure 1: The proposed model applies a common-grid time representation with a time period length of Δt and the present time point defined as time point 0.

3.2. Process network representation

We consider a process network consisting of processes that are connected by material nodes, which represent potential storage units for feeds, intermediate products, and final products. The arcs in such a network depict the directions of the material flows. Two or more streams entering the same material node are of the same quality, i.e. same chemical, temperature, pressure, etc. Figure 2 shows an example of such a process network, in which the process and material nodes are denoted by rectangles and circles, respectively.

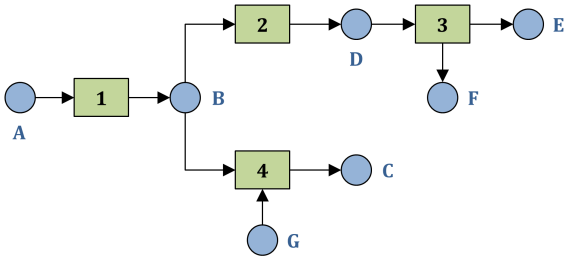

Figure 2: This example shows a simple process network consisting of process nodes (rectangles), material nodes (circles), and arcs depicting the material flows.

3.3. Mass balance constraints

For a given process network operating continuously in each time interval t, the mass balance constraints can be stated as follows:

$$Q_{jt} = Q_{j,t-1} + \sum_{i \in \hat{I}_j} P_{ijt} - \sum_{i \in \bar{I}_j} P_{ijt} + W_{jt} - D_{jt} \qquad \forall\, j,\, t \in \overline{T} \tag{1a}$$

$$Q_j^l \le Q_{jt} \le Q_j^u \qquad \forall\, j,\, t \in \overline{T} \tag{1b}$$

$$W_{jt} \le W_j^u \qquad \forall\, j,\, t \in \overline{T} \tag{1c}$$

where Q_{jt} is the inventory level for material j at time t, and P_{ijt} is the amount of material j consumed or produced by process i in time period t. $\hat{I}_j$ denotes the set of processes producing material j, whereas $\bar{I}_j$ is the set of processes receiving

material j. The additional purchase of material j in time period t is denoted by W_{jt}. The parameter D_{jt} denotes the demand for material j in time period t. Eq. (1a) states that the inventory level of a material increases when it is produced or purchased, and the inventory level decreases when the material is consumed by other processes or used to meet product demand. Eq. (1b) sets lower and upper bounds on the inventory levels. For nonstorable materials, Q_j^l and Q_j^u are zero. Eq. (1c) limits the amount of material that can be purchased.

3.4. Process surrogate model

In addition to the mass balance constraints that reflect the structure of the process network, we require a model for each individual process that relates the process' input to its output materials and expresses its capacity. Furthermore, for every feasible operating point, we have to know the amount of power required so that it can be included in the objective function. In other words, a description of each process' feasible operating region is required in the space of its input and output materials, and a power consumption correlation that is a function of those inputs and outputs.

In this framework, it is assumed that each process can operate in different operating modes. Each mode represents a particular operating state, e.g. "off", "on", or "startup". In the proposed model, the feasible operating region for each mode is defined by a union of convex subregions in the corresponding material space, and a linear power consumption function with respect to the production rates is given for each subregion. The key feature here is that every subregion has the form of a polytope. Figure 3 shows an illustrative example of the feasible operating region of a process in a two-dimensional material space. In this case, the materials are P1 and P2, and the process can operate in three different modes, Modes 1, 2, and 3. The feasible space of Mode 1 is a single point at the origin, which denotes zero production; thus, this mode is the "off" mode. The feasible space of Mode 2 is described by one single polytope, while Mode 3 is captured by the union of two polytopes, 3a and 3b. Note that the feasible regions of different modes may overlap as it is the case here for Modes 2 and 3.

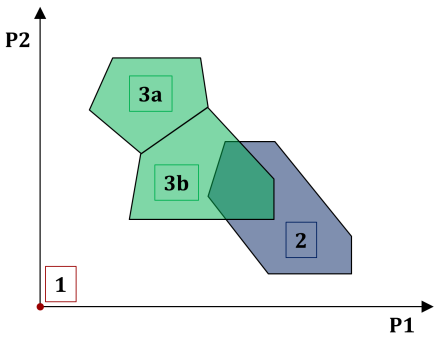

Figure 3: This illustrative example shows the feasible operating region of a process that can operate in three different operating modes.

Obviously, the feasible region of a real process typically does not have this polyhedral form. Usually, this is an approximation of the true feasible region. However, as it will be shown in the following, this representation allows us to formulate in a uniform manner models for each process, which are computationally efficient when embedded in an MILP scheduling model. Such a model is generally referred to as a Convex Region Surrogate (CRS) model. For complex processes, CRS models can be constructed by either using a model-based (Sung and Maravelias, 2009) or a data-driven approach (Zhang et al., 2014a).

Physically, at any point in time, a process can only run in one operating mode. For a given operating mode, the operating point has to lie in either one of the convex subregions. Any point in a subregion can be represented as a convex combination of the vertices of the polytope. These relationships can be expressed by the following nested disjunction:

$$\bigvee_{m \in M_i} \left[\begin{array}{c} Y_{imt} \\ \bigvee_{r \in R_{im}} \left(\begin{array}{c} \overline{Y}_{imrt} \\ P_{ijt} = \sum_{l \in L_{imr}} \lambda_{imrlt}\, \phi_{imrlj} \quad \forall\, j \in J_i \\ \sum_{l \in L_{imr}} \lambda_{imrlt} = 1 \\ 0 \le \lambda_{imrlt} \le 1 \quad \forall\, l \in L_{imr} \\ U_{it} = \delta_{imr} + \sum_{j \in J_i} \gamma_{imrj}\, P_{ijt} \end{array} \right) \end{array} \right] \quad \forall\, i,\, t \in \overline{T} \tag{2a}$$

$$\veebar_{m \in M_i} Y_{imt} \quad \forall\, i,\, t \in \overline{T} \tag{2b}$$

$$Y_{imt} \Leftrightarrow \veebar_{r \in R_{im}} \overline{Y}_{imrt} \quad \forall\, i,\, m \in M_i,\, t \in \overline{T} \tag{2c}$$

$$Y_{imt} \in \{true,\, false\} \quad \forall\, i,\, m \in M_i,\, t \in \overline{T} \tag{2d}$$

$$\overline{Y}_{imrt} \in \{true,\, false\} \quad \forall\, i,\, m \in M_i,\, r \in R_{im},\, t \in \overline{T} \tag{2e}$$

where M_i is the set of modes in which process i can operate, R_{im} is the set of operating subregions in mode $m \in M_i$, L_{imr} is the set of vertices of subregion $r \in R_{im}$, and J_i is the set of input and output materials of process i. Y_{imt} and $\overline{Y}_{imrt}$ are boolean variables. Y_{imt} is true if mode $m \in M_i$ is selected in time period t, whereas $\overline{Y}_{imrt}$ is true if subregion $r \in R_{im}$ is selected in time period t. The argument of the inner disjunction in (2a) states that the amount of material $j \in J_i$ consumed or produced by process i, P_{ijt}, is expressed as a convex combination of the corresponding vertices, ϕ_{imrlj}, while the amount of power consumed, U_{it}, is a linear function of P_{ijt} with a constant δ_{imr} and coefficients γ_{imrj} specific to the selected subregion. Eq. (2b) states that one and only one mode has to be selected for each process in each time period, and according to Eq. (2c), one region in R_{im} has to be selected if process i operates in mode $m \in M_i$.

By applying the hull reformulation (Grossmann and Trespalacios, 2013), the disjunction given by Eqs. (2) can be transformed into the following set of

mixed-integer linear constraints:

$$P_{ijt} = \sum_{m \in M_i} \sum_{r \in R_{im}} \overline{P}_{imrjt} \quad \forall\, i,\, j \in J_i,\, t \in \overline{T} \tag{3a}$$

$$\overline{P}_{imrjt} = \sum_{l \in L_{imr}} \lambda_{imrlt}\, \phi_{imrlj} \quad \forall\, i,\, m \in M_i,\, r \in R_{im},\, j \in J_i,\, t \in \overline{T} \tag{3b}$$

$$\sum_{l \in L_{imr}} \lambda_{imrlt} = \bar{y}_{imrt} \quad \forall\, i,\, m \in M_i,\, r \in R_{im},\, t \in \overline{T} \tag{3c}$$

$$U_{it} = \sum_{m \in M_i} \sum_{r \in R_{im}} \left(\delta_{imr}\, \bar{y}_{imrt} + \sum_{j \in J_i} \gamma_{imrj}\, \overline{P}_{imrjt} \right) \quad \forall\, i,\, t \in \overline{T} \tag{3d}$$

$$y_{imt} = \sum_{r \in R_{im}} \bar{y}_{imrt} \quad \forall\, i,\, m \in M_i,\, t \in \overline{T} \tag{3e}$$

$$\sum_{m \in M_i} y_{imt} = 1 \quad \forall\, i,\, t \in \overline{T} \tag{3f}$$

where y_{imt} and $\bar{y}_{imrt}$ are binary variables, and $\overline{P}_{imrjt}$ is the disaggregated variable. For each i, $j \in J_i$, $t \in \overline{T}$, only one $\overline{P}_{imrjt}$ can be nonzero.

3.5. Transition constraints

A transition occurs when the system changes from one operating point to another. For changes between operating points belonging to the same operating mode, a bound on the rate of change, Δ^u_{imj}, can be set with Eq. (4).

$$-\Delta^u_{imj} \le \sum_{r \in R_{im}} \left(\overline{P}_{imrjt} - \overline{P}_{imrj,t-1} \right) \le \Delta^u_{imj} \quad \forall\, i,\, m \in M_i,\, j \in J_i,\, t \in \overline{T} \tag{4}$$

Additional constraints have to be imposed on transitions between different modes. The dynamics of a process in terms of its mode transition behavior can be visualized with a mode transition graph. Figure 4 shows an example with four different operating modes: off, on, startup, and shutdown. The arcs in the graph show the directions of the allowed transitions with the corresponding operational constraints. For instance, after shutting down the process, i.e. transitioning from the shutdown to the off mode, the process has to remain for at least 24 hours in the off mode before it can move to the startup mode. This constraint is typically imposed to reduce stress on the equipment or plant and to account for additional costs associated with shutdowns. According to the mode transition graph, the startup phase takes exactly 4 hours before the process moves into its normal production mode, in which it then has to remain for at least 48 hours.

Eqs. (5)–(7), which model the transition constraints, are adopted from Mitra et al. (2012, 2013). Here, $z_{imm't}$ is a binary variable which is 1 if and only if process i switches from mode m to mode m' at time t, which is enforced by the following constraint:

$$\sum_{m' \in TR^f_{im}} z_{im'm,t-1} - \sum_{m' \in TR^t_{im}} z_{imm',t-1} = y_{imt} - y_{im,t-1} \quad \forall\, i,\, m \in M_i,\, t \in \overline{T} \tag{5}$$

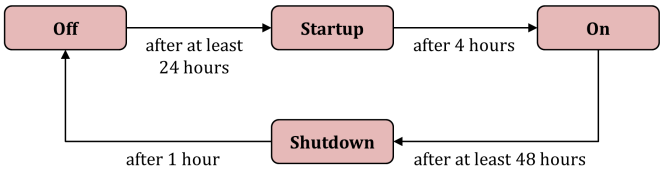

Figure 4: The mode transition graph shows the different operating modes and all possible transitions with the corresponding operational constraints.

where $TR^f_{im} = \{m' : (m', m) \in TR_i\}$ and $TR^t_{im} = \{m' : (m, m') \in TR_i\}$ with TR_i being the set of all possible mode-to-mode transitions for process i.

The restriction that a process has to remain in a certain mode for a minimum amount of time after a transition is expressed by the following constraint:

$$y_{im't} \geq \sum_{k=1}^{\theta_{imm'}} z_{imm',t-k} \quad \forall\, i,\, (m, m') \in TR_i,\, t \in \overline{T} \tag{6}$$

with $\theta_{imm'}$ being the minimum stay time in mode m' after switching to it from mode m.

For predefined sequences, each defined as a fixed chain of transitions from mode m to mode m' to mode m'', we can specify a fixed stay time in mode m' by imposing the following constraint:

$$z_{imm',t-\bar{\theta}_{imm'm''}} = z_{im'm''t} \quad \forall\, i,\, (m, m', m'') \in SQ_i,\, t \in \overline{T} \tag{7}$$

where SQ_i is the set of predefined sequences and $\bar{\theta}_{imm'm''}$ is the fixed stay time in mode m' in the corresponding sequence. For instance, in the example shown in Figure 4, this constraint applies to the sequence off-to-startup-to-on. Since the startup process takes a certain amount of time, we can use Eq. (7) to fix the number of time periods in which the process has to remain in this mode once selected.

3.6. Energy balance constraints

The required amount of electricity can be purchased from multiple sources, which is expressed in Eq. (8a). We generally refer to the different power sources as power contracts, denoted by index c. Eq. (8b) sets lower and upper bounds on the power purchase from contract c in time period t, E_{ct}. The lower bound, E^l_{ct}, is typically zero, but could be nonzero if the contract conditions demand a minimum purchase.

$$\sum_i U_{it} = \sum_c E_{ct} \qquad \forall\, t \in \overline{T} \tag{8a}$$

$$E^l_{ct} \leq E_{ct} \leq E^u_{ct} \qquad \forall\, c,\, t \in \overline{T} \tag{8b}$$

3.7. Power contract model

Eqs. (8) are sufficient if power is only purchased from the spot market or from contracts that are merely defined by a unit price for each time period and possibly some minimum and maximum purchasing restrictions. However, large industrial electricity consumers typically commit themselves to power contracts that provide additional favorable conditions. There are a large variety of such power contract structures; in this model, we consider the two most common types: discount and penalty contracts. With a discount contract, the price decreases with increasing amount of purchased power. For penalty contracts, the electricity consumer agrees to either purchase at least a certain amount of power and pay a penalty for underconsumption, or purchase not more than a certain amount to avoid penalty for overconsumption.

Discount prices and penalties are defined with respect to the amount of power purchased over a certain period of time, which could be hours, days, or even weeks. In practice, this means that the cumulative power consumption is recorded, and there are predefined meter reading times at which the amount of power purchased since the last meter reading is computed. According to this cumulative power consumption between consecutive meter readings, discount prices and penalties are issued. In our model, we track the cumulative power consumption by using the following equations:

$$F_{ct} = F_{c,t-1} + E_{ct} \qquad \forall\, c \in \overline{C},\, t \in \overline{T} \setminus \widehat{T}_c \tag{9a}$$

$$F_{ct} = F_{c,t-1} + E_{ct} - G_{ct} \qquad \forall\, c \in \overline{C},\, t \in \widehat{T}_c \tag{9b}$$

$$F_{ct} = 0 \qquad \forall\, c \in \overline{C},\, t \in \left\{0, \widehat{T}_c\right\} \tag{9c}$$

where $\overline{C}$ is the set of discount and penalty contracts and $\widehat{T}_c$ is the set of meter reading times for contract c, which does not include time 0. F_{ct} denotes the cumulative power consumption, which is set back to zero at every meter reading time. We further introduce the variable G_{ct}, which is the cumulative power consumption since the last meter reading before time t. To further clarify the notation, Figure 5 shows an illustrative example in which the cumulative power consumption meter readings are conducted every four time periods.

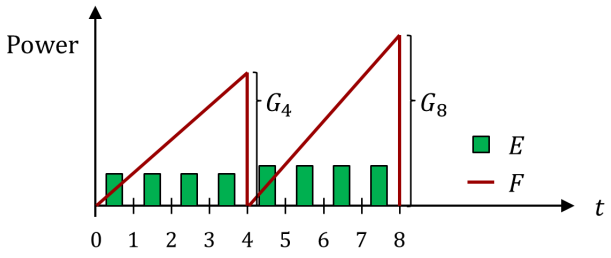

Figure 5: In this illustrative example, the cumulative power consumption meter is read every four hours.

To model discount and penalty contracts, we develop a block contract formulation that can accommodate both types of contracts. In a general block contract, each block is defined by an electricity price and the corresponding amount of power that one has to purchase in order to reach this block. In the case of a discount contract, the price decreases with each block as illustrated in Figure 6.

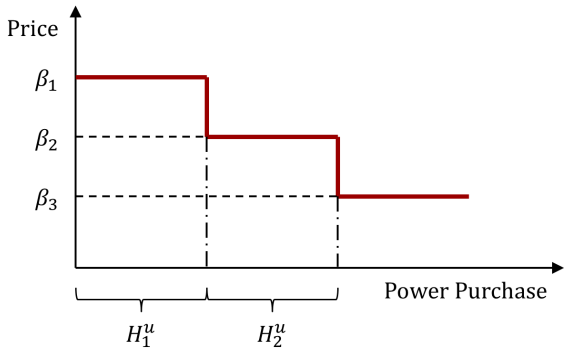

Figure 6: With a discount contract, the price decreases with increasing power purchase. The ranges for the different prices define the contract blocks.

The following disjunction expresses the mechanism of a block contract:

$$\bigvee_{b \in B_c} \begin{bmatrix} X_{cbt} \\ H_{cb't} = H^u_{cb'} \quad \forall\, b' \in B_c,\, b' < b \\ H_{cb} \leq H^u_{cb} \\ H_{cb't} = 0 \quad \forall\, b' \in B_c,\, b' > b \end{bmatrix} \qquad \forall\, c \in \overline{C},\, t \in \widehat{T}_c \tag{10a}$$

$$\bigvee_{b \in B_c} X_{cbt} \qquad \forall\, c \in \overline{C},\, t \in \widehat{T}_c \tag{10b}$$

$$X_{cbt} \in \{true,\, false\} \qquad \forall\, c \in \overline{C},\, b \in B_c,\, t \in \widehat{T}_c \tag{10c}$$

where B_c is the set of blocks for contract c, H_{cbt} denotes the amount of cumulative power purchased in block $b \in B_c$ at time t, and H^u_{cb} is the amount of power that one has to purchase in block $b \in B_c$ before reaching the next block. X_{cbt} is a boolean variable that is true if block b is the highest block reached for contract c at time t. Disjunction (10a) states that if X_{cbt} is true, the maximum amount is purchased in all lower blocks $b' < b$, the power purchase in block b is bounded by H^u_{cb}, and no power is purchased in higher blocks $b' > b$. According to logic constraint (10b), one and only one X_{cbt} has to be true.

Again, by applying the hull reformulation, Eqs. (10) can be transformed into the following mixed-integer linear constraints:

$$\sum_{b \in B_c} x_{cbt} = 1 \qquad \forall\, c \in \overline{C},\, t \in \widehat{T}_c \tag{11a}$$

$$\overline{H}_{cb'bt} = H^u_{cb'}\, x_{cbt} \qquad \forall\, c \in \overline{C},\, b \in B_c,\, b' \in B_c,\, b' < b,\, t \in \widehat{T}_c \tag{11b}$$

$$\overline{H}_{cbbt} \le H^u_{cb}\, x_{cbt} \qquad \forall\, c \in \overline{C},\, b \in B_c,\, t \in \widehat{T}_c \tag{11c}$$

$$H_{cbt} = \sum_{b' \in B_c, b' \ge b} \overline{H}_{cbb't} \qquad \forall\, c \in \overline{C},\, b \in B_c,\, t \in \widehat{T}_c \tag{11d}$$

where x_{cbt} is a binary variable, and $\overline{H}_{cbb't}$ is the disaggregated variable.

To obtain the amount of power purchased from a contract, we sum up the power purchased in all corresponding contract blocks, as stated in Eq. (12).

$$G_{ct} = \sum_{b \in B_c} H_{cbt} \quad \forall\, c \in \overline{C},\, t \in \widehat{T}_c \tag{12}$$

We can use the same block contract formulation to model penalty contracts by specifying H^u_{cb} such that the first block (Block 1) and the last block (Block $|B_c|$) correspond to under- and overconsumption, respectively. A simple penalty contract is illustrated in Figure 7. Here, if $H_{cbt} < H^u_{cb}$ for $b = 1$, we underconsume, whereas if $H_{cbt} > 0$ for $b = 3$, we overconsume.

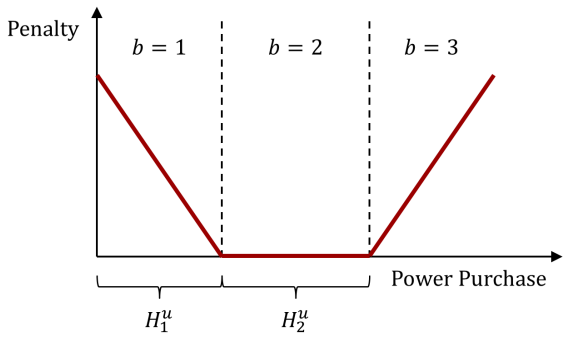

Figure 7: A simple penalty contract can be modeled as a three-block contract, with the first block and third block corresponding to under- and overconsumption, respectively.

3.8. Boundary conditions

We solve the scheduling problem for a given time horizon. For the problem to be well-defined, boundary conditions are required. The following initial conditions set the initial inventory levels, the initial operating modes, and the mode switching history:

$$Q_{j,0} = Q^i_j \qquad \forall\, j \tag{13a}$$

$$y_{im,0} = y^i_{im} \qquad \forall\, i,\, m \in M_i \tag{13b}$$

$$z_{imm't} = z^i_{imm't} \qquad \forall\, i,\, (m,m') \in TR_i,\, -\theta^u_i + 1 \le t \le -1 \tag{13c}$$

with $\theta^u_i = \max\left(\max_{(m,m') \in TR_i} \{\theta_{imm'}\}, \max_{(m,m',m'') \in SQ_i} \{\bar{\theta}_{imm'm''}\} \right)$, which defines for how far back in the past the mode switching information has to be provided.

In the following terminal constraints, we simply set lower bounds on the final inventory levels.

$$Q_{j,t^f} \geq Q_j^f \quad \forall\, j \tag{14}$$

3.9. Objective function

The objective is to minimize the total electricity cost, TC, as expressed in the following objective function:

$$TC = \sum_c \sum_{t \in \overline{T}} \alpha_{ct}\, E_{ct} + \sum_{c \in \overline{C}} \sum_{t \in \widehat{T}_c} \left[\sum_{b \in B_c} \beta_{cbt}\, H_{cbt} + \zeta_{ct}^U (H_{c,1}^u - H_{c,1,t}) + \zeta_{ct}^O\, H_{c,|B_c|,t} \right] \tag{15}$$

where α_{ct} and β_{cbt} are unit costs for purchased electricity, whereas ζ_{ct}^U and ζ_{ct}^O are unit penalty costs for under- and overconsumption, respectively. The first term in Eq. (15) represents the base cost and applies to all contracts while the remaining terms only apply to block contracts.

Note that the price structure of a contract is defined by the cost coefficients α_{ct}, β_{cbt}, ζ_{ct}^U, ζ_{ct}^O, as well as H_{cb}^u. Many combinations are possible, which provides the flexibility of modeling various different power contracts. Some common examples are listed in the following:

- Day-ahead or real-time market: $\alpha_{ct} > 0$, $\beta_{ct} = 0$, $\zeta_{ct}^U = 0$, $\zeta_{ct}^O = 0$
- Pure discount contract: $\alpha_{ct} = 0$, $\beta_{ct} > 0$, $\zeta_{ct}^U = 0$, $\zeta_{ct}^O = 0$
- Contract with partial price discount: $\alpha_{ct} > 0$, $\beta_{ct} > 0$, $\zeta_{ct}^U = 0$, $\zeta_{ct}^O = 0$
- Contract with penalty for underconsumption: $\alpha_{ct} > 0$, $\beta_{ct} = 0$, $\zeta_{ct}^U > 0$, $\zeta_{ct}^O = 0$
- Contract with penalty for overconsumption: $\alpha_{ct} > 0$, $\beta_{ct} = 0$, $\zeta_{ct}^U = 0$, $\zeta_{ct}^O > 0$
- Contract with penalties for under- and overconsumption: $\alpha_{ct} > 0$, $\beta_{ct} = 0$, $\zeta_{ct}^U > 0$, $\zeta_{ct}^O > 0$
- Combined discount and penalty contract: $\alpha_{ct} > 0$, $\beta_{ct} > 0$, $\zeta_{ct}^U > 0$, $\zeta_{ct}^O > 0$

By considering the objective function given by Eq. (15), it is assumed that electricity cost constitutes the vast majority of the operating cost or that other costs required to satisfy the given demand are constant. If this assumption is invalid and additional costs—such as inventory costs, mode transition costs, and costs of purchasing material—need to be considered, they can be easily incorporated by assigning cost coefficients to the corresponding variables.

4. Illustrative example

To demonstrate the main features of the model, we first apply it to an illustrative example for which the process network is shown in Figure 8.

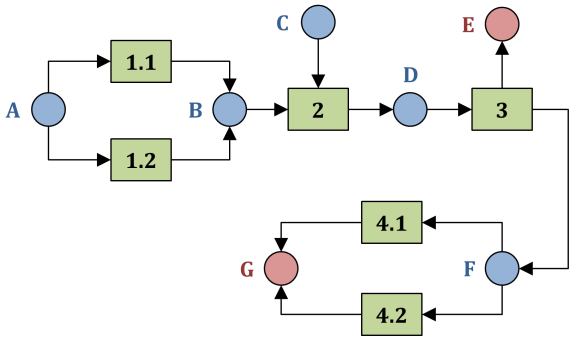

Figure 8: The process network of the illustrative example consists of four process and seven material nodes.

Each process is characterized by its operating modes and operating subregions. The vertices of each convex subregion are listed in Table 1 where each vertex is given as a vector of the materials. Note that the on mode of Process 3 is the only mode that is described by two subregions. Each operating subregion is further characterized by a linear power consumption function, which is shown in Table 2. Possible transitions between different operating modes and predefined sequences are listed in Tables 3 and 4, respectively; the tables also contain the corresponding minimum and fixed stay times given in hours. No bound is imposed on the rate of change in the same mode.

Table 1: Vertices associated with each operating subregion of the processes from the illustrative example.

Process	Mode	Region	Vertex	A	B	C	D	E	F	G
1.1	off	1	1	0	0	0	0	0	0	0
	on	1	1	60	60	0	0	0	0	0
			2	600	600	0	0	0	0	0
1.2	off	1	1	0	0	0	0	0	0	0
	on	1	1	20	20	0	0	0	0	0
			2	200	200	0	0	0	0	0
2	off	1	1	0	0	0	0	0	0	0
	startup	1	1	0	0	0	0	0	0	0
	shutdown	1	1	0	0	0	0	0	0	0
	on	1	1	0	40	20	60	0	0	0
			2	0	800	4000	1200	0	0	0
3	off	1	1	0	0	0	0	0	0	0
	startup	1	1	0	0	0	0	0	0	0
	shutdown	1	1	0	0	0	0	0	0	0
	on	1	1	0	0	0	100	50	50	0
			2	0	0	0	100	45	55	0
			3	0	0	0	1000	500	500	0
			4	0	0	0	1000	450	550	0
		2	1	0	0	0	100	45	55	0
			2	0	0	0	100	40	60	0
			3	0	0	0	1000	450	550	0
			4	0	0	0	1000	400	600	0
4.1	off	1	1	0	0	0	0	0	0	0
	on	1	1	0	0	0	0	0	30	30
			2	0	0	0	0	0	300	300
4.2	off	1	1	0	0	0	0	0	0	0
	on	1	1	0	0	0	0	0	30	30
			2	0	0	0	0	0	300	300

Table 2: Power consumption correlations associated with each operating subregion. Each correlation is a linear function of the materials.

Process	Mode	Region	Power Consumption Correlation
1.1	off	1	0
	on	1	500 + 2A
1.2	off	1	0
	on	1	450 + 3A
2	off	1	0
	startup	1	200
	shutdown	1	150
	on	1	100 + 0.5D
3	off	1	0
	startup	1	400
	shutdown	1	200
	on	1	800 + 3D
	on	2	1000 + 4D
4.1	off	1	0
	on	1	400 + 2F
4.2	off	1	0
	on	1	350 + 1.5F

Table 3: Possible transitions between the different operating modes of each process and the corresponding minimum stay times.

Process	Transition from Mode m to Mode m'	Minimum Stay Time in Mode m'
1.1	off → on	0
	on → off	0
1.2	off → on	0
	on → off	0
2	off → startup	1
	startup → on	6
	on → shutdown	1
	shutdown → off	6
3	off → startup	2
	startup → on	6
	on → shutdown	1
	shutdown → off	12
4.1	off → on	0
	on → off	0
4.2	off → on	0
	on → off	0

Table 4: Predefined sequences of mode transitions and the corresponding fixed stay times.

Process	Sequence (Transition from m to m' to m'')	Fixed Stay Time in m'
2	off → startup → on	1
	on → shutdown → off	1
3	off → startup → on	2
	on → shutdown → off	1

Data regarding the inventory of each material are given in Table 5. Infinite availability of feedstock, A and C, is assumed. Also note that Intermediate B is not storable. Moreover, no material can be purchased, i.e. $W_j^u = 0 \ \forall j$.

Table 5: Inventory bounds and initial inventory levels for each material.

	A	B	C	D	E	F	G
Minimum Inventory	0	0	0	0	3,000	0	5,000
Maximum Inventory	∞	0	∞	8,000	20,000	2,000	30,000
Initial Inventory	∞	0	∞	800	5,000	0	8,000
Minimum Final Inventory	0	0	0	800	5,000	0	8,000

We consider a two-day scheduling horizon with an hourly time discretization. The results for three different product demand scenarios (low, high, and medium) will be compared; the corresponding demand profiles are shown in Figure 9. Note that in the low and high demand scenarios, the demands for E and G are constant over time while they vary in the medium demand scenario.

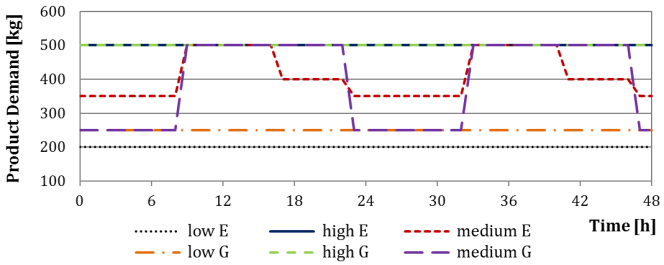

Figure 9: Product demand profiles for the three different scenarios (low, high, and medium).

Three different power contracts are considered: a time-of-use (TOU), a discount, and a penalty contract. The base electricity price profiles for each of the contracts are shown in Figure 10. Other features differentiating the three contracts are the following:

- The TOU contract does not have any additional price components.
- With the discount contract, the additional cost depends on the purchased amount of power over the course of each day, i.e. the cumulative power consumption meter is read at the end of each day. For the first 50 MWh, an additional cost of 10 \$/MWh needs to be paid; for the next 40 MWh, a cost of 8 \$/MWh occurs; and for any amount of power purchased beyond 90 MWh, the cost is 5 \$/MWh.
- With the penalty contract, penalties are applied to under- as well as over-consumption. A penalty of 50 \$/MWh has to be paid if the daily power purchase from the penalty contract is below 20 MWh or exceeds 80 MWh. Otherwise, there is no cost in addition to the base cost.

Moreover, when applied, the maximum amount that can be purchased from each contract every hour is 10 MWh.

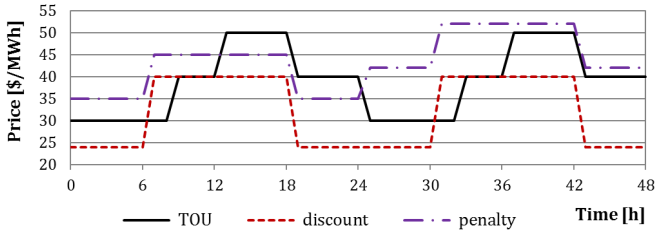

Figure 10: Base electricity prices for each of the three different power contracts.

Using the data from the illustrative example, we now consider five cases which differ in the product demand and the applied power contracts as shown in Table 6. In all cases, all processes are in the on mode at the start of the scheduling horizon. Also, it is assumed that no mode switching has occurred in the previous 12 hours. The total electricity costs in each case obtained by solving the MILP model are listed in the last column of Table 6.

Table 6: The table lists the five cases, which differ in the product demands and in the power contracts, with the optimal total electricity costs.

Case	Product Demand	Power Contracts	Total Electricity Cost
1	low	TOU	$ 5,771
2	high	TOU	$ 14,624
3	medium	TOU	$ 11,697
4	medium	TOU, discount	$ 11,057
5	medium	TOU, penalty	$ 11,346

For Case 1, the optimal schedule is shown in Figure 11, which depicts a Gantt chart showing the operating modes of each process in each time period. Figure 12 shows the amount of power consumed by each process. Also, one can observe that the plant is shut down for a large portion of the time, primarily when the electricity price is high. This large shift in load is possible due to the low demand and the flexibility in the inventory as indicated by the changes in inventory levels shown in Figure 13. Also note that for the conversion of A to B, Process 1.1 is preferred over Process 1.2 due to its higher capacity and lower unit power consumption. Similarly, Process 4.2 is preferred over Process 4.1 due to its higher efficiency.

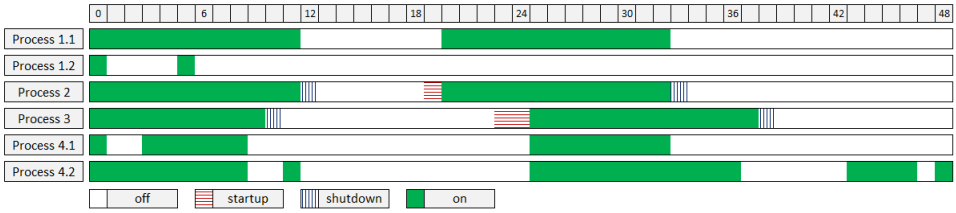

Figure 11: Gantt chart for the optimal schedule in Case 1. Selected operating modes of each process are shown for each time period.

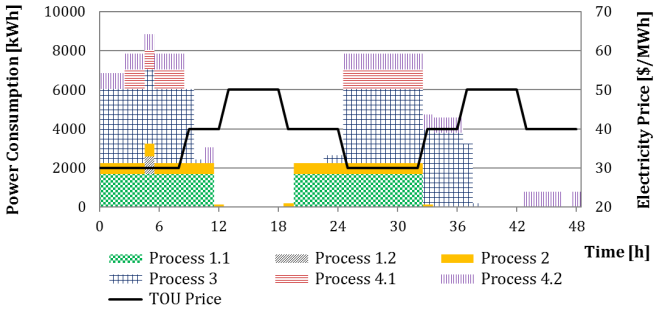

Figure 12: Amount of power consumed by each process in Case 1.

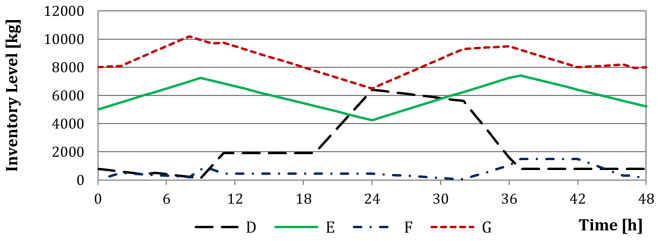

Figure 13: Inventory profiles of the intermediate materials D and F, and the final products E and G in Case 1.

The power consumption profiles in Case 2 are shown in Figure 14, which only expresses moderate load shifting. This can be explained by the reduced level of process flexibility due to the high demand. Here, the plant has to utilize almost its entire production capacity to satisfy demand. Figure 15 shows the result for Case 3, which indicates that with medium time-varying demand, there is again significant potential for load shifting.

In Case 4, the discount contract is applied in addition to the TOU contract. Figure 16 shows the breakdown of the total power purchase into the purchases

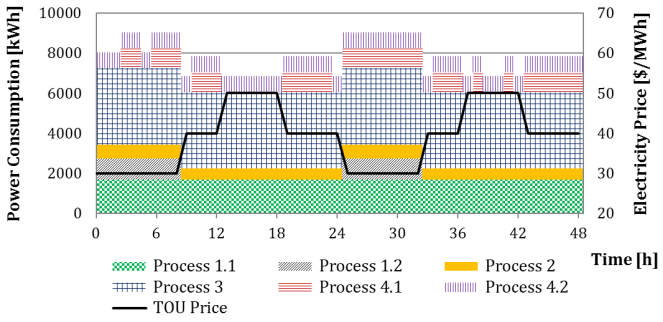

Figure 14: Amount of power consumed by each process in Case 2.

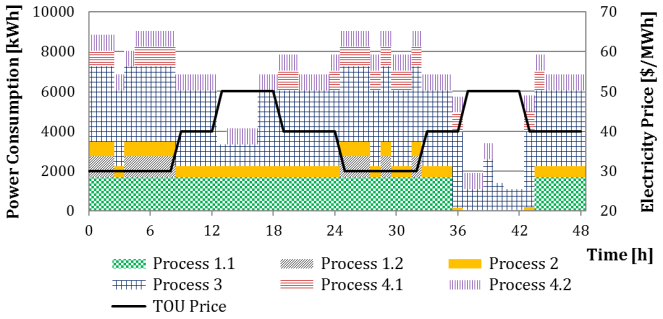

Figure 15: Amount of power consumed by each process in Case 3.

from these two contracts and the base prices. The majority of the consumed power in the first 24 hours, namely 135.5 MWh, is purchased from the discount contract. By doing so, we are taking advantage of the best possible discount. However, there are still time periods in which the TOU contract offers a lower price. In those hours, power is purchased from the TOU contract. On the second day, 53.9 MWh are purchased from the discount contract. We would purchase more from the discount contract for a larger discount; however, the threshold for that discount is too high for this to be beneficial. Therefore, the rest of the consumed power is purchased from the TOU contract.

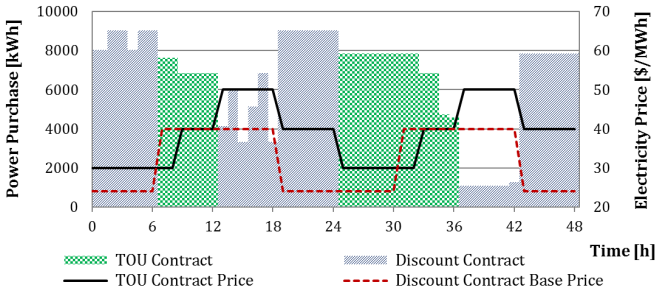

Figure 16: Breakdown of the total electricity purchase into the purchases from the TOU and the discount contracts in Case 4.

In Case 5, the TOU and the penalty contracts are applied. Figure 17 shows the breakdown of the total power purchase and the base prices. Notice that the price for the penalty contract is higher on the second day. 80 MWh and 20 MWh are purchased from the penalty contract on the first and second day, respectively. It is clear that because of the low price on the first day, we try to purchase as much as possible from the penalty contract without having to pay any penalties. On the second day, since the price is now high, we purchase just enough to avoid penalties.

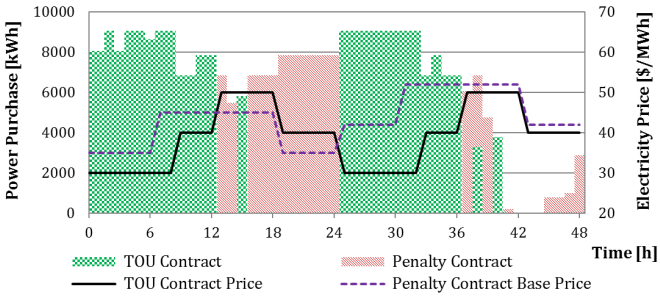

Figure 17: Breakdown of the total electricity purchase into the purchases from the TOU and the penalty contracts in Case 5.

All models were implemented in GAMS 24.4.1 (GAMS Development Corporation, 2015), and the commercial solver CPLEX 12.6.1 has been applied to solve the MILPs. In each case, the model has approximately 5,000 continuous variables, 2,500 binary variables, and 7,500 constraints. All models have been solved to zero integrality gap in less than 20 seconds wall-clock time on an Intel® Core™ i7-2600 machine at 3.40 GHz with eight processors and 8 GB RAM running Windows 7 Professional.

5. Industrial case study

We now apply the proposed model to a real-world industrial case study provided by Praxair. Here, we consider an air separation plant that produces gaseous oxygen (GO2), gaseous nitrogen (GN2), liquid oxygen (LO2), liquid nitrogen (LN2), and liquid argon (LAr). The corresponding process network is shown in Figure 18. The GO2, LO2, LN2, and LAr flowing out of the air separation (AS) process can be directly sold whereas GN2 has to be further compressed before it can be sent to the pipelines. Two kinds of GN2 are sold: medium-pressure GN2 (MPGN2) and high-pressure GN2 (HPGN2). GN2 is compressed to MPGN2 through Process LMCompGN2 and can be further compressed to HPGN2 through Process MHCompGN2; it can also be directly converted to HPGN2 by running Process LHCompGN2. Furthermore, GN2 can be liquefied to LN2 by running Process LiqGN2. Overproduced gaseous products can be vented through a venting process, and all liquid products can be converted into the corresponding gaseous products through a so-called driox process.

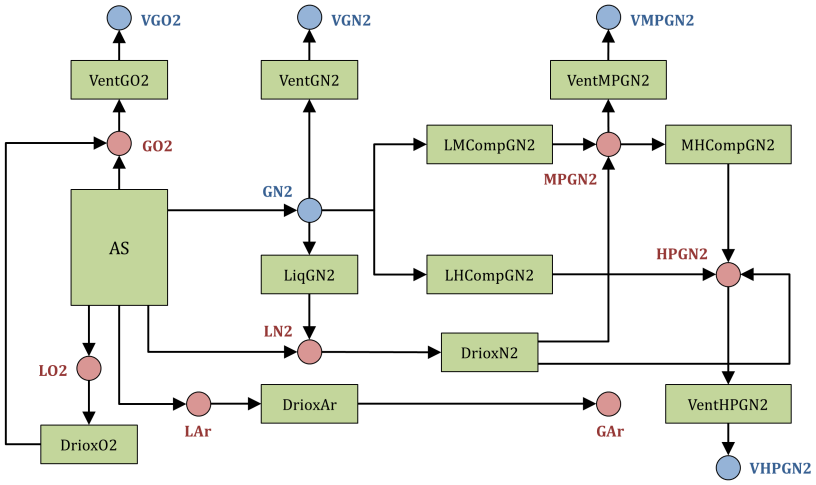

Figure 18: Process network representing the given air separation plant.

While there are inventories of the liquid products, we assume that gaseous products cannot be stored. Power can be purchased from three different sources: a TOU contract, a penalty contract, and the spot market. While pre-agreed prices for the TOU and the penalty contracts are known, a forecast of the hourly-varying spot price is used in the model. For the penalty contract, penalties are only paid for underconsumption.

The scheduling horizon is one week, to which an hourly time discretization is applied resulting in 168 time periods. Demand profiles for all products are given. Note that while there is continuous demand for gaseous products, the demand for each liquid product is assumed to occur only at the end of each day. The assumption here is that there is sufficient flexibility in the inventory

to handle flows into and out of the inventory tank throughout the day. The demand at the end of the day is then the total amount of product that needs to be drawn from the tank over the course of the day.

We solve the resulting MILP model to obtain the optimal schedule. Please note that due to confidentiality reasons, we cannot disclose information about the plant specifications as well as the actual product demand. Therefore, all results presented in the following are given without units and rescaled if necessary. However, the analysis and interpretation of the results is still meaningful.

Figure 19 shows the power consumption profiles for each of the processes. The vast majority of the power consumption is attributed to the air separation unit (ASU). The GN2 liquefier also consumes a large amount of power but is only used five times, each time for a few hours. Compared to the ASU and the GN2 liquefier, the pipeline compressors contribute relatively little to the total power consumption. Significant load shifting can be observed in the schedule; this is mainly realized by operating the liquefier during low-price hours, which allows a fairly constant operation of the other processes.

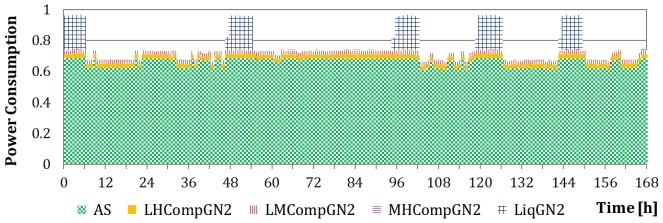

Figure 19: Amount of power consumed by each process of the air separation plant.

The breakdown of the total power purchase into the purchases from the three different sources as well as the corresponding electricity prices are shown in Figure 20. One can observe that in each time period, we choose to purchase from the source with the lowest price. Two sources are chosen in the same time period only when the maximum purchase amount is reached for one of the two sources. Also, sufficient amount of power is purchased from the penalty contract such that no penalty has to be paid.

As an example, Figure 21 shows the amount of GN2 produced by the AS process and the GN2 flows into the subsequent processes. Large portion of GN2 is compressed to feed the product pipelines. Another significant amount of GN2 is liquefied to increase the production of LN2. However, the majority of GN2 is vented. The reason for this overproduction of GN2 is that the plant is "oxygen-limited", which means that the production is driven by the oxygen demand. At such a plant, the nitrogen production usually exceeds the demand, which makes venting of GN2 necessary.

Figure 22 shows the flows into and out of the LN2 inventory tank and the resulting inventory profile. LN2 flowing out of the ASU and the liquefier increases the inventory while LN2 used for driox and demand, i.e. LN2 draws from the

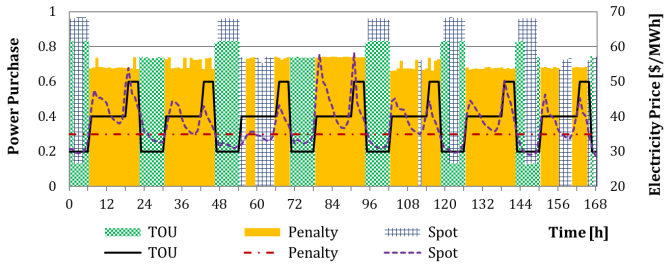

Figure 20: Breakdown of the total electricity purchase into the purchases from the three difference sources.

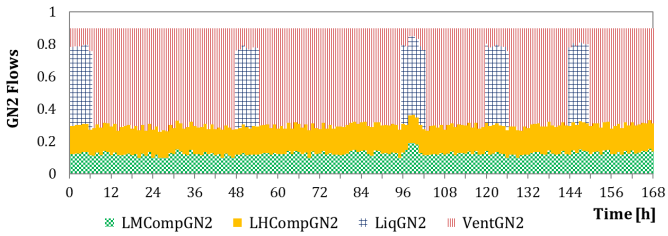

Figure 21: GN2 production and its breakdown into feeds for different processes.

tank, decrease the inventory. One can see that demand occurs every 24 hours. In addition to the production through the AS process, large amount of LN2 is obtained by liquefying GN2. Driox is used only very sporadically.

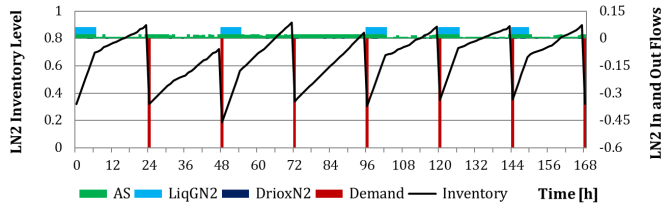

Figure 22: LN2 flows and inventory profile.

The MILP model for the industrial-scale problem has 28,808 continuous variables, 9,776 binary variables, and 113,810 constraints. It has been solved to zero integrality gap in 7 seconds wall-clock time on the same Intel® Core™ i7-2600 machine used to solve the illustrative example. A brief computational study has been conducted by solving several instances of the problem with different input parameters. Almost all instances have been solved within two minutes.

6. Conclusions

In this work, a general discrete-time MILP model has been developed for the scheduling of continuous power-intensive process networks with various power contracts. The main focus of the proposed formulation are the accurate and efficient representation of the operational flexibility in the production process as well as the modeling of power contracts. A process network has been considered where each process is represented by a Convex Region Surrogate model. A mode-based formulation has been adopted to model operational transitions. Moreover, a block formulation has been proposed that allows the modeling of a large variety of power contracts including commonly occurring discount and penalty contracts.

The proposed scheduling model has been applied to an illustrative example as well as to a real-world air separation plant. The results demonstrate the capability of the model in representing the operation of continuous process networks and the flexibility in modeling different power contracts. This allows the optimal scheduling of power-intensive processes involving load shifting within the feasible range of operation. Furthermore, the proposed MILP model has proven to be computationally very efficient. Large-scale problems with tens of thousands of variables and hundreds of thousands of constraints can be solved within a few minutes, which allows the use of such a scheduling tool in a real industrial setting.

Nomenclature

Indices

b, b'	contract blocks
c	power contracts
i	processes
j	materials
l	vertices
m, m', m''	operating modes
r	(convex) operating subregions
t	time periods

Sets

B_c	contract blocks for block contract c
C	power contracts
$\overline{C}$	block contracts, i.e. discount and penalty contracts, $\overline{C} \subseteq C$
I	processes
$\bar{I}_j$	processes receiving material from material j
$\hat{I}_j$	processes producing material in material j
J_i	materials associated with process i, $J_i = \bar{J}_i \cup \hat{J}_i$

$\bar{J}_i$	materials that are inputs to process i
$\hat{J}_i$	materials that are outputs of process i
L_{imr}	vertices of subregion r in mode m of process i
M_i	modes for process i
R_{im}	subregions in mode m of process i
SQ_i	predefined sequences of mode transitions in process i
T	time periods, $T = \{-\theta^u + 1, -\theta^u + 2, \ldots, 0, 1, \ldots, t^f\}$
$\overline{T}$	time periods in the scheduling horizon, $\overline{T} = \{1, 2, \ldots, t^f\}$
$\widehat{T}_c$	cumulative power consumption meter reading times for contract c
TR_i	possible mode transitions in process i
TR_{im}^f	modes of process i from which mode m can be directly reached
TR_{im}^t	modes of process i which can be directly reached from mode m

Parameters

D_{jt}	demand for material j in time period t [kg]
E_{ct}^u	maximum amount of power that can be purchased from contract c in time period t [kWh]
H_{cb}^u	maximum cumulative power purchased in block b of contract c [kWh]
Q_j^f	minimum final inventory level for material j [kg]
Q_j^i	initial inventory level for material j [kg]
Q_j^l	minimum inventory level for material j [kg]
Q_j^u	maximum inventory level for material j [kg]
W_j^u	maximum purchasing amount for material j [kg]
y_{im}^i	1 if process i was operating in mode m in time period 0
$z_{imm't}^i$	1 if operation of process i switched from mode m to mode m' at time t before time 0
α_{ct}	base unit price for power purchased from contract c in time period t [\$/kWh]
β_{cbt}	additional unit price for cumulative power purchased from block b of contract c at time t [\$/kWh]
γ_{imrj}	unit power consumption corresponding to material j if process i operates in subregion r of mode m [kWh/kg]
δ_{imr}	fixed power consumption if process i operates in subregion r of mode m [kWh]
Δ_{imj}^u	maximum rate of change in the amount of material j consumed or produced in mode m of process i [kg]
ζ_{ct}^O	unit overconsumption penalty cost for contract c at time t [\$/kWh]
ζ_{ct}^U	unit underconsumption penalty cost for contract c at time t [\$/kWh]
$\theta_{imm'}$	minimum stay time in mode m' after switching from mode m to mode m' in process i [Δt]
θ^u	largest minimum stay time [Δt]

$\bar{\theta}_{imm'm''}$	fixed stay time in mode m' in the predefined sequence (m, m', m'') in process i $[\Delta t]$
ϕ_{imrlj}	amount of material j associated with vertex l of subregion r in mode m of process i [kg]

Continuous Variables

E_{ct}	power purchased from contract c in time period t [kWh]
F_{ct}	cumulative power purchased from contract c at time t [kWh]
G_{ct}	cumulative power purchased from contract c at meter reading time t [kWh]
H_{cbt}	cumulative power purchased in block c of contract c at meter reading time t [kWh]
$\overline{H}_{cbb't}$	diaggregated variable for H_{cbt} corresponding to block/disjunct b' [kWh]
P_{ijt}	amount of material j consumed or produced by process i in time period t [kg]
$\overline{P}_{imrjt}$	amount of material j consumed or produced in subregion r of mode m of process i in time period t [kg]
Q_{jt}	inventory level for material j at time t [kg]
TC	total electricity cost [$]
U_{it}	power consumed by process i in time period t [kWh]
W_{jt}	amount of material in material j purchased in time period t [kg]
λ_{imrlt}	coefficient for vertex l of subregion r in mode m of process i in time period t

Binary Variables

x_{cbt}	1 if block b is the highest block reached for of contract c at time t
y_{imt}	1 if process i operates in mode m in time period t
$\bar{y}_{imrt}$	1 if process j operates in subregion r of mode m in time period t
$z_{imm't}$	1 if process i switches from mode m to mode m' at time t

Acknowledgements

The authors gratefully acknowledge the financial support from the National Science Foundation under Grant No. 1159443 and from Praxair.

References

Albadi, M. H., El-Saadany, E. F., Nov. 2008. A summary of demand response in electricity markets. Electric Power Systems Research 78 (11), 1989–1996.

Ashok, S., May 2006. Peak-load management in steel plants. Applied Energy 83 (5), 413–424.

Babu, C., Ashok, S., May 2008. Peak Load Management in Electrolytic Process Industries. IEEE Transactions on Power Systems 23 (2), 399–405.

Castro, P. M., Harjunkoski, I., Grossmann, I. E., Jul. 2009. New Continuous-Time Scheduling Formulation for Continuous Plants under Variable Electricity Cost. Industrial & Engineering Chemistry Research 48 (14), 6701–6714.

Castro, P. M., Harjunkoski, I., Grossmann, I. E., Feb. 2011. Optimal scheduling of continuous plants with energy constraints. Computers & Chemical Engineering 35 (2), 372–387.

Castro, P. M., Sun, L., Harjunkoski, I., 2013. Resource-Task Network Formulations for Industrial Demand Side Management of a Steel Plant. Industrial & Engineering Chemistry Research 52, 13046–13058.

Charles River Assosicates, 2005. Primer on Demand-Side Management. Tech. Rep. February, The World Bank.

GAMS Development Corporation, 2015. GAMS version 24.4.1.

Grossmann, I. E., Trespalacios, F., 2013. Systematic Modeling of Discrete-Continuous Optimization Models through Generalized Disjunctive Programming. AIChE Journal 59 (9), 3276–3295.

Harjunkoski, I., Maravelias, C. T., Bongers, P., Castro, P. M., Engell, S., Grossmann, I. E., Hooker, J., Méndez, C., Sand, G., Wassick, J., Mar. 2014. Scope for industrial applications of production scheduling models and solution methods. Computers & Chemical Engineering 62, 161–193.

Ierapetritou, M. G., Wu, D., Vin, J., Sweeney, P., Chigirinskiy, M., Oct. 2002. Cost Minimization in an Energy-Intensive Plant Using Mathematical Programming Approaches. Industrial & Engineering Chemistry Research 41 (21), 5262–5277.

Karwan, M. H., Keblis, M. F., Mar. 2007. Operations planning with real time pricing of a primary input. Computers & Operations Research 34 (3), 848–867.

Kondili, E., Pantelides, C. C., Sargent, R. W. H., 1993. A General Algorithm for Short-Term Scheduling of Batch Operations - I. MILP Formulation. Computers & Chemical Engineering 17 (2), 211–227.

Maravelias, C. T., 2012. General Framework and Modeling Approach Classification for Chemical Production Scheduling. AIChE Journal 58 (6), 1812–1828.

Méndez, C. A., Cerdá, J., Grossmann, I. E., Harjunkoski, I., Fahl, M., May 2006. State-of-the-art review of optimization methods for short-term scheduling of batch processes. Computers & Chemical Engineering 30 (6-7), 913–946.

Merkert, L., Harjunkoski, I., Isaksson, A., Säynevirta, S., Saarela, A., Sand, G., Jun. 2014. Scheduling and energy – Industrial challenges and opportunities. Computers & Chemical Engineering 72, 183–198.

Mitra, S., Grossmann, I. E., Pinto, J. M., Arora, N., Mar. 2012. Optimal production planning under time-sensitive electricity prices for continuous power-intensive processes. Computers & Chemical Engineering 38, 171–184.

Mitra, S., Sun, L., Grossmann, I. E., Jun. 2013. Optimal scheduling of industrial combined heat and power plants under time-sensitive electricity prices. Energy 54, 194–211.

Pantelides, C. C., 1994. Unified Frameworks for Optimal Process Planning and Scheduling. In: Foundations of computer-aided process operations. New York, pp. 253–274.

Paulus, M., Borggrefe, F., Feb. 2011. The potential of demand-side management in energy-intensive industries for electricity markets in Germany. Applied Energy 88 (2), 432–441.

Samad, T., Kiliccote, S., Dec. 2012. Smart grid technologies and applications for the industrial sector. Computers & Chemical Engineering 47, 76–84.

Shah, N., Pantelides, C., Sargent, R., Feb. 1993. A general algorithm for short-term scheduling of batch operations - II. Computational issues. Computers & Chemical Engineering 17 (2), 229–244.

Sung, C., Maravelias, C. T., 2009. A Projection-Based Method for Production Planning of Multiproduct Facilities. AIChE Journal 55 (10), 2614–2630.

Vujanic, R., Mariéthos, S., Goulart, P., Morari, M., 2012. Robust Integer Optimization and Scheduling Problems for Large Electricity Consumers. In: 2012 American Control Conference. pp. 3108–3113.

Zhang, Q., Grossmann, I. E., Sundaramoorthy, A., Pinto, J. M., 2014a. Data-driven construction of Convex Region Surrogate models (submitted for publication).

Zhang, Q., Heuberger, C. F., Grossmann, I. E., Sundaramoorthy, A., Pinto, J. M., 2014b. Air Separation with Cryogenic Energy Storage: Optimal Scheduling Considering Electric Energy and Reserve Markets (to appear in AIChE Journal).